

Flocculation of Deformable Emulsion Droplets

II. Interaction Energy

DIMITER N. PETSEV, NIKOLAI D. DENKOV, AND PETER A. KRALCHEVSKY¹

Laboratory of Thermodynamics and Physicochemical Hydrodynamics, Faculty of Chemistry, University of Sofia, 1126 Sofia, Bulgaria

Received September 28, 1994; accepted March 9, 1995

The effect of different factors (drop radius, interfacial tension, Hamaker constant, electrolyte, micellar concentrations, etc.) on the interaction energy of emulsion droplets is studied theoretically. It is demonstrated that the deformation of the colliding droplets considerably affects the interaction energy. The contributions of the electrostatic, van der Waals, depletion, steric, and oscillatory surface forces, as well as of the surface stretching and bending energies, are estimated and discussed. The calculations show that the droplets interact as nondeformed spheres when the attractive interactions are weak. At stronger attractions an equilibrium plane parallel film is formed between the droplets, corresponding to minimum interaction energy of the system. For droplets in concentrated micellar surfactant solutions the oscillatory surface forces become operative and one can observe several minima of the energy surface, each corresponding to a metastable state with a different number of micellar layers inside the film formed between the droplets. The present theoretical analysis can find applications in predicting the behavior and stability of miniemulsions (containing micrometer and submicrometer droplets), as well as in interpretation of data obtained by light scattering, phase behavior, rheological and osmotic pressure measurements, etc. © 1995 Academic Press, Inc.

Key Words: emulsion, flocculation in; thin liquid films; radial distribution function, in miniemulsions; depletion interaction; oscillatory surface force; bending energy, in emulsions; interaction energy, between emulsion drops.

1. INTRODUCTION

In the first part of this study (1) we analyzed the shape of two droplets forming an equilibrium doublet in emulsion. The result, obtained using the augmented Laplace equation (2), was compared with a model shape (plane parallel film between spherical droplets—Fig. 1) which was used in previous studies on droplet interactions (3, 4) and coalescence (5). The comparison shows that the interaction energies

between two deformed droplets, calculated using the actual and model shapes, are in good agreement. This enables one to perform easily (by using the simple model shape) extensive numerical calculations in order to reveal the effect of different factors on the behavior of an emulsion consisting of deformable droplets. Such numerical studies can be carried out for large macroemulsion droplets (above 1 μm) as well as for small Brownian miniemulsion droplets (below 1 μm).

There is some experimental evidence that the deformability may affect the overall equilibrium properties of emulsions. By using optical microscopy and contact angle measurements, Aronson and Princen (6) observed that single drops coexist with aggregates of droplets. In fact, the aggregates are flocculated droplets separated by thin liquid films. It has been established that the three-phase contact angle (and the film area) increase with increasing the electrolyte concentration and decreasing the temperature in these experiments. Hofman and Stein (7) studied experimentally the flocculation of emulsions containing very small (of micrometer size) droplets and have explained some of the results with the possible droplet deformation at certain conditions (high ionic strength and low interfacial tension). A similar idea was proposed to explain some experimental results obtained with microemulsions (8).

A method for producing miniemulsions consisting of fairly monodisperse droplets was recently proposed (9). This method allows quantitative experimental investigation of the interdroplet interaction and its effect on the miniemulsion properties—phase diagrams, structure factor, kinetics of flocculation, etc. The present study provides an approach which can be used to interpret experimental data from miniemulsion studies.

In general, the present article extends and develops the ideas and methods proposed in the preceding studies, Refs. (3, 4). It was shown in Ref. (3) that the energy of interaction between two deformed emulsion droplets, W , depends on two geometrical parameters, the film thickness, h , and the film radius, r , i.e., $W = W(h, r)$; see Fig. 1 for notation.

¹ To whom correspondence should be addressed. E-mail: Peter.Kralchevsky@Ltpf.cit.bg.

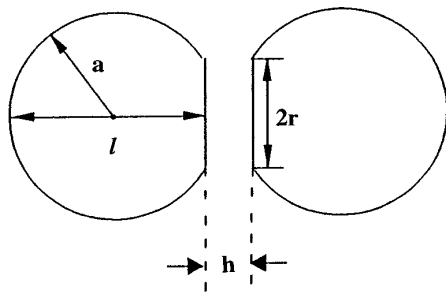


FIG. 1. Sketch of two deformed droplets (the film thickness and radius are exaggerated).

On the other hand, one expects to see the interaction energy W as a function of the distance z between the droplets' mass centers, i.e., $W = W(z)$. Some *approximate* relations for $h(z)$ and $r(z)$ have been accepted in Ref. (3) in order to estimate $W(z) = W(h(z), r(z))$.

The *rigorous* theoretical approach to this problem was formulated in Ref. (4). In this approach, the dependence of the interaction energy on the interparticle interaction is characterized by the potential of the mean force $w_f(z) = -kT \ln g(z)$, where k is the Boltzmann constant, T is temperature, and $g(z)$ is the pair (radial) correlation function. The crucial point is that $g(z)$ is determined by *statistical averaging* over all possible droplet configurations (of different values of h and r) corresponding to a given z :

$$g(z) = \frac{4}{\Gamma(1/4)} \left(\frac{\pi a^2 \gamma}{2kT} \right)^{1/4} \times \frac{1}{a} \int \exp \{ -W[h(r), r]/kT \} dr. \quad [1.1]$$

Here $\Gamma(x)$ is the gamma function, $\Gamma(1/4) = 3.625\ 609\ 908\ .\ .\ .$; a and γ are the droplet radius and interfacial tension; $h(r)$ represents the geometrical relation between h and r at fixed z . One sees that a prerequisite for calculating $w_f(z)$ is the knowledge of the function $W(h, r)$. A model expression for $W(h, r)$, based on the DLVO theory, was used in Ref. (4) to illustrate the proposed general approach.

The present article meets the need for a comprehensive study of the physical consequences and applications of the general concept from Ref. (4) to emulsion systems in which droplet–droplet interactions of various kinds are operative. The study is focused on the calculation of $W(h, r)$ for different combinations of surface forces; it is an extension and development over Refs. (3, 4) in the following aspects:

(1) The onset of droplet deformation and the equilibrium film radius are studied as functions of electrolyte concentration and droplet size.

(2) The contribution in $W(h, r)$ of various non-DLVO surface forces (depletion, oscillatory, structural, steric) is examined; the cases when nonionic and ionic surfactant micelles are present in the continuous phase are studied separately and compared.

(3) In addition to the energy of interfacial *stretching* upon droplet collision, the energy of interfacial *bending* is also taken into account. We note in advance that the bending energy gives a contribution on the order of $10\ kT$ to the total droplet–droplet interaction and turns out to be an important effect.

Since most of the studied factors (droplet radius, electrolyte concentration, Hamaker constant, presence of ionic or nonionic micelles, etc.) are subject to experimental control, our analysis allows one to prevent (or induce, if necessary) *flocculation* in a given emulsion system. In this respect the present paper is complementary to Ref. (5) which deals with *coalescence* of deformable droplets. The results are relevant also to flocs, containing more than two particles, because in most cases the theory predicts small or moderate deformation and pairwise additivity of the interaction energy.

2. SURFACE EXTENSION ENERGY AND DLVO SURFACE FORCES

The electrostatic and van der Waals interactions are accounted for by the DLVO theory in its conventional form (10–12). In the case of *deformable droplets* the surface extension energy should be also taken into account. We begin with a brief consideration of these three contributions to the total interaction energy.

The van der Waals interactions between two deformed drops of equal size can be quantified by means of Eq. [2.2] in Ref. (1). In most cases an accurate approximate expression (for moderate deformations and separations) can be used:

$$W^{\text{vw}}(h, r) = -\frac{A_H}{12} \left[\frac{3}{4} + \frac{a}{h} + 2 \ln \left(\frac{h}{a} \right) + \frac{r^2}{h^2} - \frac{2r^2}{ah} \right],$$

for $\frac{h}{a} < 0.3, \frac{r}{a} < 0.5$. [2.1]

More general expressions for arbitrarily deformed spheres of different sizes (as well as for a deformed sphere and a wall) are given in Ref. (3).

The electrostatic interactions, however, can hardly be presented in an explicit manner in the general case. Still, some accurate approximate expressions could be derived (3). Thus, in the case of weak double layer overlap (which corre-

sponds to the nonlinear superposition approximation (10, 13)) one can use the formula (3)

$$f(h) = B \exp\left(-\frac{h}{\sigma}\right), \quad [2.2]$$

$$W = \pi r^2 f(h) + \pi a \int_h^\infty f(H) dH, \quad [2.3]$$

where $\sigma = \kappa^{-1}$ (for 1:1 electrolyte) and

$$B = 64 kTC_{\text{EL}}\kappa^{-1} \tanh^2\left(\frac{e\Psi_0}{4kT}\right),$$

$$\kappa^2 = \frac{2e^2}{\epsilon_0\epsilon kT} C_{\text{EL}} \quad [2.4]$$

defines the Debye screening parameter. C_{EL} is the electrolyte number concentration and Ψ_0 is the electric potential of the drop surface. This approximation can be used in most cases for Brownian particles (3–5). If the requirement for weak double layer overlap is violated, the expression [2.2] for $f(h)$ is not already applicable, but when the particle surface potential is low (below 25 mV) one can use other formulas for the electrostatic interaction energy derived in Refs. (3, 5). For deformable particles of high surface potentials at small separations, numerical calculations are needed to calculate $f(h)$; they can be performed as explained in Refs. (3, 10–12).

By combining Eqs. [2.2]–[2.4], one obtains the following expression for the interaction energy between two identical deformed droplets (1, 3, 4):

$$W^{\text{EL}}(h, r) = \frac{64\pi C_{\text{EL}}kT}{\kappa} \tanh^2\left(\frac{e\Psi_0}{4kT}\right) \times \exp(-\kappa h) \left[r^2 + \frac{a}{\kappa} \right]. \quad [2.5]$$

Summing up Eqs. [2.1] and [2.5] and the expression for the surface extension energy (1, 3, 5)

$$W^{\text{S}}(r) = \gamma \frac{\pi r^4}{2 a^2}, \quad \text{for } \left(\frac{r}{a}\right)^2 \ll 1, \quad [2.6]$$

one may calculate the total energy of interaction between two deformed droplets.

In Fig. 2a the contour plot of the energy of interaction between two droplets is shown as a function of the interparticle spacing h and the film radius r . The droplet radius a is chosen to be 1 μm , the surface potential is $\Psi_0 = 100$ mV,

the interfacial tension is $\gamma = 1$ mN/m, the electrolyte concentration is $C_{\text{EL}} = 0.1$ M, and the Hamaker constant is $A_{\text{H}} = 2 \times 10^{-20}$ J (14, 15). The minimum of the potential surface is $W(h_e, r_e)/kT = -60.1$, and corresponds to an *equilibrium* doublet of two droplets at distance $h_e/a = 0.0076$ with film radius $r_e/a = 0.076$. The ordinate axis ($r = 0$) crosssection corresponds to the case of nondeformable particles with the minimum of the interaction energy equal to $W(h^*, 0)/kT = -51.1$ at $h^*/a = 0.0062$.

A decrease of the Hamaker constant (keeping all the remaining parameters unchanged) leads to a weaker deformation; see Fig. 2b. In this case the Hamaker constant is $A_{\text{H}} = 10^{-20}$ J and the minimum of the interaction energy $W(h_e, r_e)/kT = -23.4$ is reached at $h_e/a = 0.0081$ and $r_e/a = 0.045$. At the ordinate axis the minimum of the energy is $W(h^*, 0)/kT = -22.69$.

Fig. 2c corresponds to the Hamaker constant $A_{\text{H}} = 5 \times 10^{-21}$ J. The local minimum is not observed, which means that a stable doublet of *deformed* droplets is missing. In fact, the minimum has degenerated into a ‘‘valley’’ whose deepest point, $W/kT = -10.2$, lies on the ordinate axis. Hence, the equilibrium droplets are spherical (nondeformed).

The dependencies of the equilibrium radius, r_e , of the film formed between two deformable droplets, and of the respective energy minimum, $W_e = W(h_e, r_e)$, on the electrolyte concentration are illustrated in Fig. 3. The Hamaker constant in this case is $A_{\text{H}} = 10^{-20}$ J, the interfacial tension is $\gamma = 1$ mN/m, and the surface potential is $\Psi_0 = 100$ mV. Fig. 3a shows the dependence of the film radius on the electrolyte concentration. The full line is for droplets with radius $a = 1$ μm , the dashed one for $a = 0.5$ μm , and the dotted one for $a = 2$ μm . It is seen that r_e is almost zero until a certain value of the electrolyte concentration is reached. At this value (which is different for the different drop sizes), r_e starts to increase sharply. Note that the smaller the droplets, the greater the electrolyte concentration needed to start the deformation. Fig. 3b illustrates how the minimum of the interaction energy, W_e , changes with the concentration of electrolyte. The dot-dashed line presents the minimum energy for nondeformed droplets, $W(h^*, 0)/kT$ with $a = 1$ μm . As might be expected, the depth of the energy minimum increases with increased electrolyte concentration. This effect is much more pronounced for deformable droplets. The differences between the energy minima for deformed and nondeformed droplets, $\Delta W_e/kT = W_e/kT - W(h^*, 0)/kT$, corresponding to different sizes (0.5, 1, and 2 μm) are presented in Fig. 3c. The effect of the droplet deformability on the interaction energy becomes substantial for electrolyte concentrations greater than, c.a., 0.1 M.

Fig. 4 gives an example of how the equilibrium film radius r_e and the energy difference $\Delta W_e/kT$ depend on the particle radius a at fixed other parameters. Fig. 4a shows the plot of

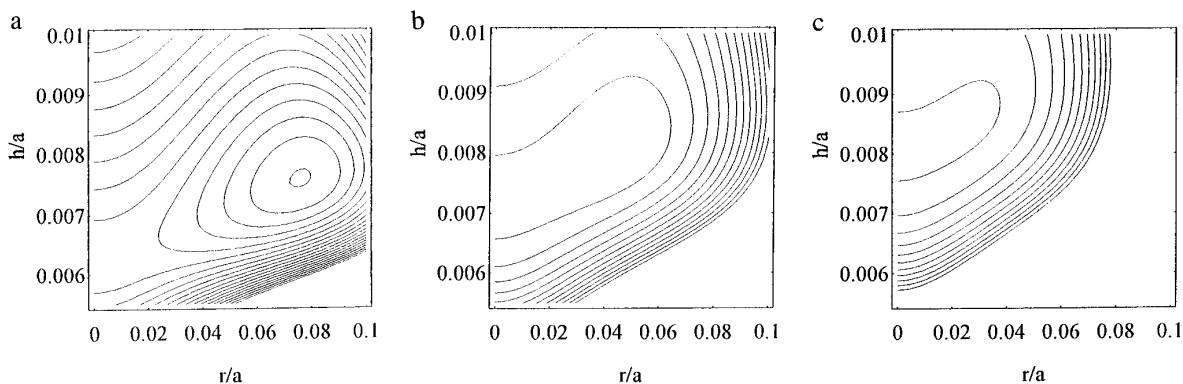


FIG. 2. Contour plot of the electrostatic and van der Waals interaction energy $W(h, r)/kT$ between two deformable droplets: $a = 1$ micrometer, $\Psi_0 = 100$ mV, $\gamma = 1$ mN/m, $C_{\text{EL}} = 0.1$ M. (a) $A_H = 2 \times 10^{-20}$ J, the minima of the energies for deformable and nondeformable droplets are $W(h_e, r_e)/kT = -60.1$ and $W(h^*, 0)/kT = -51.1$ respectively. The distance between two contours equals $2 kT$; (b) $A_H = 1 \times 10^{-20}$ J, the minima of the energies for deformable and nondeformable droplets are $W(h_e, r_e)/kT = -23.4$ and $W(h^*, 0)/kT = -22.7$ respectively. The distance between two contours equals $2 kT$; (c) $A_H = 5 \times 10^{-21}$ J, the minima of the energies for deformable and nondeformable droplets are $W(h_e, r_e)/kT = -10.2$. The distance between two contours equals $1 kT$.

the film radius vs droplet radius; the solid line corresponds to electrolyte concentration 0.1 M and the dashed one to 0.05 M. The remaining parameters are the same as in Fig. 2a. It is seen that the film radius (normalized by the droplet radius) is initially rather small, then it sharply increases, and finally levels off. This shape of the r_e vs a dependence is due to the

fact that $|W^{\text{VW}}| \ll W^{\text{EL}} + W^{\text{S}}$ for small droplets, whereas $|W^{\text{VW}}| \gg W^{\text{EL}} + W^{\text{S}}$ for larger droplets. The small values of r_e/a and h_e/a justify the applicability of Eq. [2.1] for the van der Waals interaction energy (the assumptions used to derive it are fulfilled). Using the expression (see Ref. (1) for details)

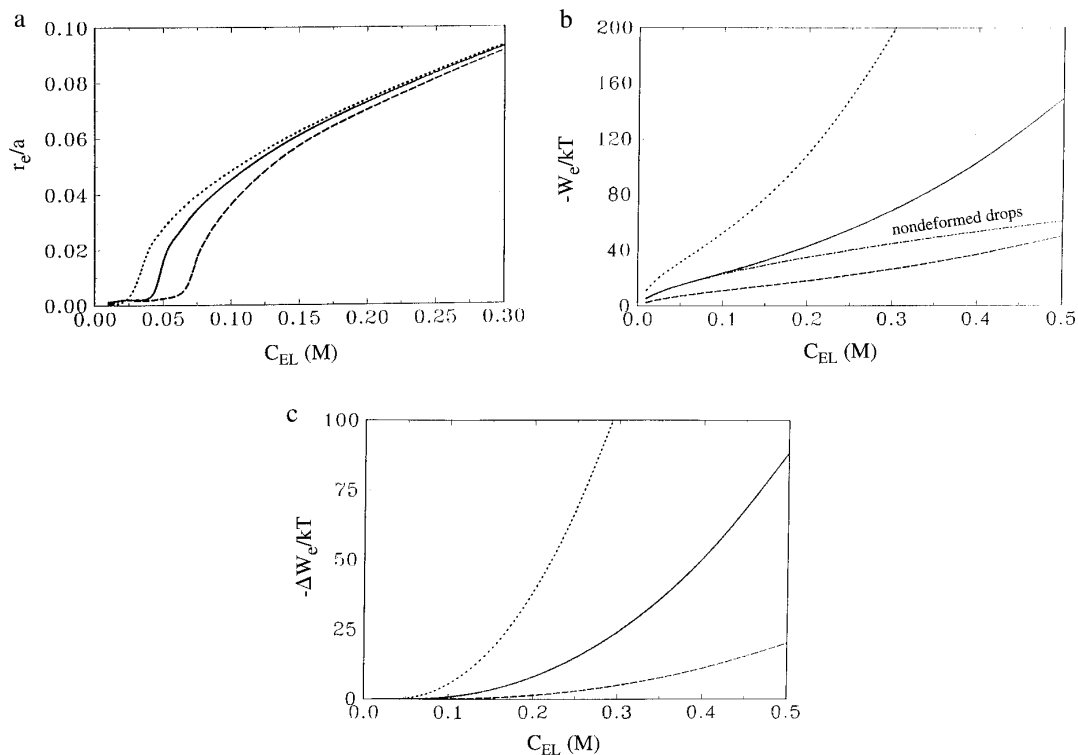


FIG. 3. Influence of the electrolyte concentration. The parameters are the same as in Fig. 2b, except those specified below. The full line corresponds to $a = 1$ micrometer, the dashed to $a = 0.5$ micrometer, and the dotted to $a = 2.0$ micrometers. (a) Normalized film radius r_e/a vs electrolyte concentration C_{EL} ; (b) Energy minima $W_e = W(h_e, r_e)/kT$ vs electrolyte concentration C_{EL} ; (c) Differences between the minima in the energies for deformable and nondeformable droplets.

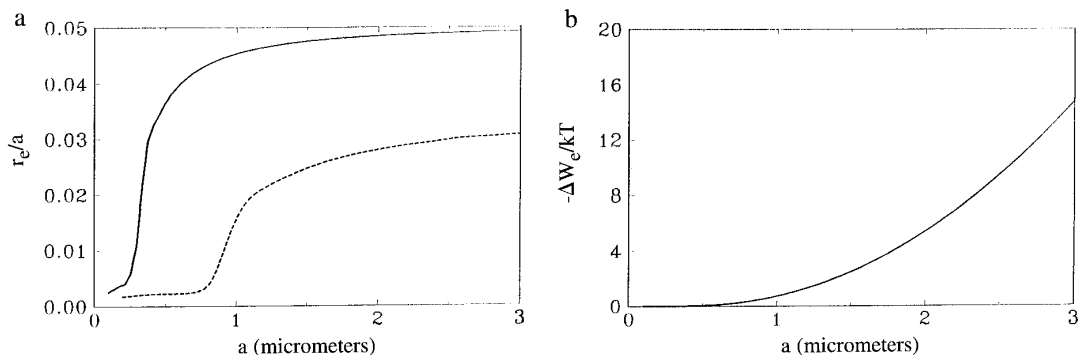


FIG. 4. Influence of the droplet size. The parameters are the same as in Fig. 2b, except those specified. (a) Normalized film radius r_e/a vs droplet radius a ; The full line corresponds to $C_{EL} = 0.1 M$ and the dashed to $C_{EL} = 0.05 M$; (b) Difference between the energy minima for deformable and nondeformable droplets for $C_{EL} = 0.1 M$.

$$\alpha_e = \arcsin \frac{r_e}{a} \quad [2.7]$$

we may calculate the equilibrium contact angle α_e ; thus we obtain $\alpha_e = 2.88^\circ$ for $C_{EL} = 0.10 M$, and $\alpha_e = 1.94^\circ$ for $C_{EL} = 0.05 M$.

The energy effect due to deformation, ΔW_e , is plotted vs a in Fig. 4b for $0.1 M$ electrolyte. One sees that the larger the droplet, the greater the energy of doublet formation.

In summary, the increase of the Hamaker constant, electrolyte concentration, and droplet size lead to a greater droplet deformation and stronger flocculation. The most intriguing finding is that under the combined action of the first two factors one can observe droplet deformation even with very small (submicrometer) droplets, whose deformability is usually neglected in the studies on emulsions, cf., Figs. 2a and 3a.

3. EFFECT OF THE NON-DLVO FORCES

During the past two decades it was established that in addition to the electrostatic and van der Waals forces, a number of other interactions could play an important role in colloid stability (3–5, 9, 13–15, 17, 18). The most popular among them seem to be the depletion interaction (due to soluble polymers or surfactant micelles present in the disperse medium) and the steric interaction (due to polymer molecules adsorbed at the drop surface). For the system under consideration all of these interactions can be usually treated in the framework of Derjaguin's approximation; see Eq. [2.2] and Ref. (1).

At higher concentrations of micelles or globular macromolecules the depletion interaction develops into the oscillatory structural forces (14, 16), which are characterized by alternate zones of attraction and repulsion. It is quite intriguing to examine how these oscillatory forces affect the

interaction between emulsion droplets (see subsection 3.2 below).

Other important non-DLVO surface forces (not considered in the present article) are ionic correlation forces, monotonic hydration repulsion, and hydrophobic attraction (14, 16). The last force should not be expected between emulsion droplets insofar as the droplet surfaces are hydrophilized by the adsorbed surfactant molecules. In contrast, the ionic correlation forces can lead to a strong droplet–droplet attraction in oil-in-water emulsions in the presence of bivalent or multivalent counterions. The hydration force can lead to a strong short-range interdroplet repulsion in the presence of strongly hydrated ions (Mg^{2+} , Li^+ , etc.). The effect of the ionic correlation and hydration forces on emulsion stability may be the subject of a subsequent study.

3.1. Depletion Interaction

If smaller colloidal species (micelles, microemulsions, polymer molecules) are present in the disperse medium, an attraction between the emulsion drops appears at small separations (4, 9, 17). This attraction has an osmotic nature and the corresponding interaction energy can generally be presented in the form

$$W_d = -P_o V_E, \quad [3.1]$$

where P_o is the osmotic pressure created by the micelles (or the polymer molecules) and V_E denotes the volume in the gap between the drops, which is excluded for the access of the smaller species; see Fig. 5.

Let us first consider the simpler case where nonionic micelles, behaving as hard spheres of diameter d , are present. Then P_o can be expressed accurately enough by the Carnahan–Starling (19) formula

$$P_o = \xi C_M kT, \quad \xi = \frac{1 + \Phi + \Phi^2 - \Phi^3}{(1 - \Phi)^3}, \quad [3.2]$$

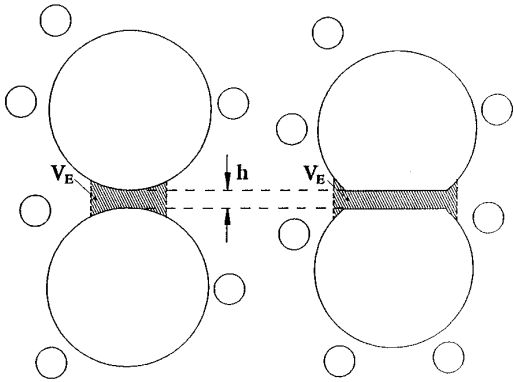


FIG. 5. Depletion effects for nondeformed and deformed droplets. Note that the excluded volume V_E is greater for deformed than for nondeformed droplets.

where C_M is the number density of the micelles and Φ is their volume fraction. The excluded volume V_E in this case is determined mostly by geometrical constraints and for two *deformed* spheres like those shown in Fig. 5 can be expressed as follows (3):

$$V_E = \pi \left[r^2(d - h) + \frac{a}{2}(d - h)^2 \right] \quad h \leq d$$

$$d/a \ll 1. \quad [3.3]$$

Following the general approach presented in Section 2 we can analyze the contribution of the depletion interaction between two deformable spheres. In Fig. 6 the contour plot of the interaction energy between two drops in the presence of nonionic micelles, $W(h, r)$, is shown (the parameters are $A_H = 10^{-20}$ J, $a = 1$ μ m, $\Psi_0 = 100$ mV, $C_{EL} = 0.1$ M, $\gamma = 1$ mN/m, $\Phi = 10\%$, and $d = 10$ nm; cf. Fig. 2b). It is seen that the attractive depletion interaction leads to a larger droplet deformation ($r_e/a = 0.064$), while the same droplets in the absence of micelles are less deformed ($r_e/a = 0.045$, Fig. 2b). The respective energy minima are $W_e/kT = -31.6$ and $W_e/kT = -23.4$.

In Fig. 7a we plot the dependencies of the equilibrium film radius on the drop radius in the presence of nonionic micelles at two different concentrations: $\Phi = 5\%$ (dashed curve) and $\Phi = 10\%$ (solid curve). Surface extension energy and van der Waals, electrostatic, and depletion interactions are taken into account in these calculations. One sees from the figure that the attractive depletion interaction increases the drop deformation—the film radius is larger for the higher micellar concentration.

In Fig. 7b the difference in the pair interaction energy (at the potential minimum) between deformed ($r > 0$) and nondeformed ($r = 0$) drops at different micellar concentra-

tions are plotted. The curves in Fig. 7b clearly show that the attraction between the deformed drops is stronger. In other words, the depletion attraction enhances the deformation, which in its own turn increases the magnitude of the pair attraction energy and facilitates the droplet flocculation. Quantitatively this follows from Eq. [3.3], which shows that V_E increases with increasing r , and consequently the interaction energy due to depletion increases with increasing droplet deformation.

In the case of ionic micelles the osmotic pressure, P_o , can be substantially different from that predicted by Eq. [3.2]. In principle, the osmotic pressure of a suspension of charged colloidal species can be calculated using some of the available theories, e.g., Ref. (20). It turned out that the experimental results for depletion interaction (and the related oscillatory structural forces; see below) obtained with stratifying foam films (21, 22) and with the surface force balance (23) could be quantitatively interpreted using a simple model. Eq. [3.2] is used again, but the actual micellar volume fraction, Φ , is replaced with an effective (larger) volume fraction, Φ_o , which includes the counterion atmosphere:

$$\Phi_o = \frac{4}{3} \pi \left(\frac{d}{2} + \kappa^{-1} \right)^3 C_M. \quad [3.4]$$

In addition, the micelles are electrostatically repelled from the drop surface, which leads to an excluded volume, V_E , larger than that predicted by Eq. [3.3]. A reasonable approximation for V_E in this case can be obtained by utilizing the idea of Richetti and Kekicheff (23), that the micelles cannot reach separations from the drop surface smaller than a certain distance b (in their experiments b was determined to be about $2.5 \kappa^{-1}$):

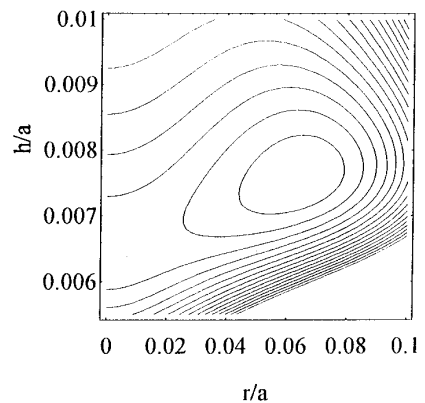


FIG. 6. Contour plot of the interaction energy including depletion interactions in the presence of nonionic micelles with volume fraction $\Phi = 0.1$. All the parameters are as in Fig. 2b, the micellar diameter is 10 nm, and the parameter $\xi = 1.52$. The energy minima are $W(h_e, r_e)/kT = -31.6$ and $W(h^*, 0)/kT = -27.4$ for deformable and nondeformable droplets, respectively. The distance between the contours equals $2 kT$.

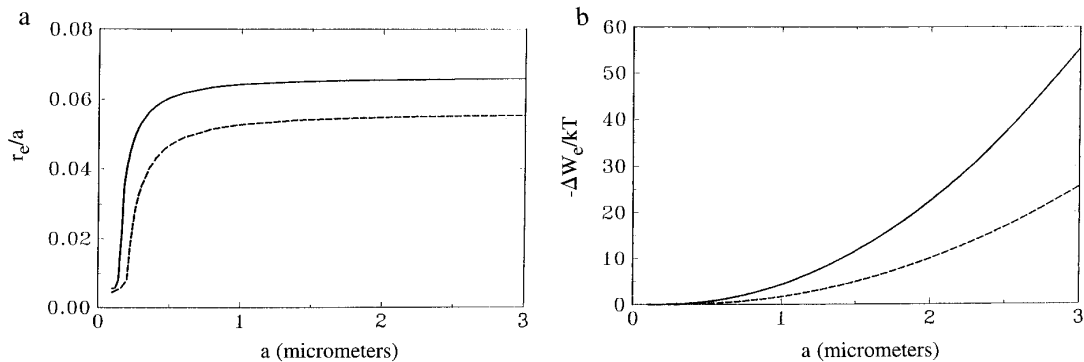


FIG. 7. Influence of the concentration of nonionic micelles on the film radius and interaction energy. The full curves corresponds to $\Phi = 0.1$ and the dashed to $\Phi = 0.05$. The corresponding values for the parameter ξ are 1.52 and 1.23. (a) Normalized film radius r_e/a vs droplet radius a ; (b) Difference between the minima in the energies for deformable and nondeformable droplets.

$$V_E = \pi \left[r^2(d + 2b - h) + \frac{a}{2} (d + 2b - h)^2 \right];$$

$$h \leq d + 2b. \quad [3.5]$$

Hence, the depletion effect due to *ionic* micelles compared to that of *nonionic* micelles is more pronounced at the same micelle number concentration and is strongly dependent on the electrolyte concentration.

3.2. Oscillatory Structural Forces

As shown experimentally by Richetti and Kekicheff (23), at higher micellar concentrations an oscillatory type force appears between two solid surfaces. For foam films the stratification (stepwise thinning of the film, in the presence of micelles or latex particles) was explained by Nikolov *et al.* (21, 22) as a layer by layer expulsion of a micellar structure formed inside the film, which is again a manifestation of the oscillatory structural forces. Since a similar effect is expected for emulsion films, below we study the effect of the oscillatory structural forces (due to micelles) on the interaction between miniemulsion droplets.

Recently, a semiempirical explicit formula for description of the oscillatory structural forces between two solid surfaces in the presence of hard spheres of diameter d was proposed (24),

$$\Pi^{\text{os}}(h) = \begin{cases} P_o \cos\left(\frac{2\pi h}{d}\right) \exp\left(1 - \frac{h}{d}\right) & \text{for } h > d \\ -P_o & \text{for } 0 \leq h \leq d, \end{cases} \quad [3.6]$$

where $\Pi^{\text{os}}(h)$ is the respective component of the disjoining pressure (the surface force per unit area of the film surfaces) and P_o is expressed by means of Eq. [3.2]. A physical

explanation of the oscillations of Π^{os} is given by Israelachvili (14) by means of the contact value theorem; see Eq. [13.4] and Fig. 13.2 in Ref. (14). In general, the maxima of Π^{os} correspond to an increased repulsion, which stabilizes the thin films. On the other hand, at low micelle volume fraction these maxima disappear and the oscillatory force degenerates into the attractive depletion force. The latter fact resolves the paradox of why the micelles (and any small colloidal particles) destabilize dispersions at lower volume fractions, but stabilize dispersions at higher volume fractions. From Eq. [3.6] and the thermodynamic relationship

$$f^{\text{os}}(h) = \int_h^\infty \Pi(H) dH, \quad [3.7]$$

one can calculate the interaction energy per unit area of a planar film due to the oscillatory forces (24):

$$f^{\text{os}}(h) = \begin{cases} P_o \frac{d \exp(1 - (h/d))}{(4\pi^2 + 1)} & h > d \\ \times \left[\cos\left(\frac{2\pi h}{d}\right) - 2\pi \sin\left(\frac{2\pi h}{d}\right) \right] & \\ P_o \left(h - d + \frac{d}{4\pi^2 + 1} \right) & 0 \leq h \leq d. \end{cases} \quad [3.8]$$

The numerical comparison with results obtained by means of the Monte Carlo (25) method or from the Percus–Yevick integral equation (26) shows that Eqs. [3.6] and [3.8] are accurate for not very low volume fractions despite of their semiempirical character (24). More accurate expressions for Π^{os} and f^{os} , accounting for the dependence of d on the volume fraction Φ , can be found in Ref. (24).

The substitution of Eq. [3.8] into Derjaguin's approxima-

tion, Eq. [2.3], leads to the following expression for the interaction energy of deformed spheres:

$$W^{os}(h, r) = \begin{cases} \pi r^2 P_o \frac{d \exp(1 - (h/d))}{(4\pi^2 + 1)} \\ \times \left[\cos\left(\frac{2\pi h}{d}\right) - 2\pi \sin\left(\frac{2\pi h}{d}\right) \right] \\ - \pi a P_o \frac{d^2 \exp(1 - (h/d))}{(4\pi^2 + 1)^2} \\ \times \left[(4\pi^2 + 1) \cos\left(\frac{2\pi h}{d}\right) + 4\pi \sin\left(\frac{2\pi h}{d}\right) \right], & h > d \\ \pi r^2 P_o \left(h - d + \frac{d}{4\pi^2 + 1} \right) \\ + \pi a P_o \frac{d^2 (4\pi^2 - 1)}{(4\pi^2 + 1)^2} \\ + \pi a P_o (d - h) \left(\frac{d}{4\pi^2 + 1} - \frac{d}{2} + \frac{h}{2} \right) & 0 \leq h \leq d. \end{cases} \quad [3.9]$$

Similarly to the case of depletion interaction, discussed in the previous subsection, the results can be extended to ionic micelles. For that purpose we include the thickness of the ionic atmosphere, κ^{-1} , to define an effective diameter of the micelles, d_o , which is larger than the actual one (21, 23):

$$d_o = d + 2/\kappa. \quad [3.10]$$

The effective micellar volume fraction, Φ_o , can be calculated from Eq. [3.4] and the osmotic pressure by means of Eq. [3.2] with $\Phi = \Phi_o$. The electrostatic repulsion between the ionic micelles and the similarly charged drop surfaces leads to a larger excluded volume for the micelles. Then, the counterpart of Eq. [3.6] can be written in the form

$$\Pi^{os}(h) = \begin{cases} P_o \cos\left[\frac{2\pi(h-2b)}{d_o}\right] \\ \times \exp\left(1 - \frac{(h-2b)}{d_o}\right); & \text{for } h > d_o + 2b \\ -P_o; & \text{for } 0 \leq h \leq d_o + 2b. \end{cases} \quad [3.11]$$

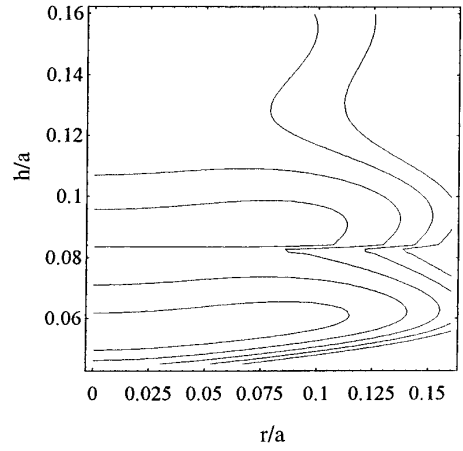


FIG. 8. Contour plot of the energy $W(h, r)/kT$ in the presence of ionic micelles. The micellar parameters are close to those known for sodium dodecylsulfate (SDS) micelles: diameter $d = 4.8$ nm, $v_a = 80$, micellar charge number 20 (degree of dissociation 25%), and critical micellar concentration $\text{CMC} = 10^{-3}$ M. The other parameters are: $\gamma = 1$ mN/m, $A_H = 10^{-20}$ J, $\Psi_0 = 100$ mV, $C_{EL} = 0.1$ M, $a = 0.1$ micrometers, $b = 1/\kappa$.

b accounts for the excluded volume in the vicinity of the film walls, due to electrostatic repulsion. The integration of Eq. [3.11] in accordance with Eq. [3.7] and Derjaguin's approximation (Eq. [2.2] in Ref. (1)) again yields Eqs. [3.8] and [3.9], in which h and d are replaced by $h - 2b$ and d_o , respectively.

From Eqs. [2.1]–[2.6], [3.2], [3.3], [3.8]–[3.10], one can calculate the total interaction energy $W(h, r)$ between two charged deformable drops in the presence of ionic micelles as a superposition of contributions due to the van der Waals, electrostatic, and oscillatory surface forces and the surface extension effect. The contour plot of $W(h, r)$ calculated in this way is shown in Fig. 8. The parameters are close to those known for sodium dodecylsulfate (SDS) micelles: diameter $d = 4.8$ nm, aggregation number $v_a = 80$, micellar charge number 20 (degree of dissociation 25%), and critical micellar concentration $\text{CMC} = 10^{-3}$ M. The other parameters are $\gamma = 1$ mN/m, $A_H = 10^{-20}$ J, $\Psi_0 = 100$ mV, $C_{EL} = 0.1$ M, and $a = 0.1$ μm . When calculating Debye length κ^{-1} we took into account both the neutral electrolyte (0.1 M NaCl) and the ions due to surfactant monomer and micelle dissociation (21, 23)

$$\kappa^2 = \frac{2e^2}{\epsilon_0 \epsilon kT} \left[C_{EL} + \text{CMC} + \frac{3\alpha v_a \Phi}{\pi d^3} \right], \quad [3.12]$$

where α is the degree of dissociation of the micelle surface ionizable groups. One sees from Fig. 8 that the presence of micelles leads to a complex shape of the energy surface which may exhibit two local minima. From the viewpoint of colloid stability, more important is the repulsion barrier

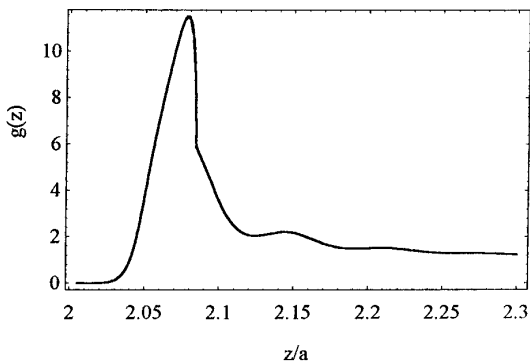


FIG. 9. Radial correlation function for droplets with the same parameters as in Fig. 8.

(separating the valleys of the two minima), which opposes the thinning of the film and the droplets coalescence. Note that even when there is not a well defined local minimum at any $r_e \neq 0$, the deformability of the droplets contributes to the radial distribution function due to the specificity of the statistical averaging; see Eq. [1.1].

As explained in the Introduction, the radial correlation function, $g(z)$, can be determined from the energy surface $W(h, r)$. $g(z)$ is plotted in Fig. 9 for deformable droplets of radius 100 nm in the presence of 0.1 M ionic surfactant and 0.1 M electrolyte. The effective volume fraction of the micelles in this case is $\Phi_o = 0.1136$ and $b = 1/\kappa$. The micellar aggregation number is assumed to be $v_a = 80$, the critical micellization concentration is $\text{CMC} = 0.001$ M, and the dissociation of the micelle surface ionizable groups is 25%. The main peak corresponds to the depletion attraction between the deformable droplets (with no micelles in the film region) while the smaller ones correspond to the presence of micelles in the gap.

3.3. Steric Interaction

In the case of steric interaction, the particular form of the interaction energy per unit area, $f^{\text{st}}(h)$, depends on the properties of the solvent in the continuous phase. At theta-conditions $f^{\text{st}}(h)$ can be calculated by means of the theory by Dolan and Edwards (27)

$$f^{\text{st}}(h) = \Gamma kT \left[\frac{\pi^2}{3} \left(\frac{L_o}{h} \right)^2 - \ln \left(\frac{8\pi}{3} \frac{L_o^2}{h^2} \right) \right] \quad \text{for } h < \sqrt{3} L_o$$

$$f^{\text{st}}(h) = 4\Gamma kT \exp \left[\left(-\frac{3}{2} \frac{h^2}{L_o^2} \right) \right] \quad \text{for } h > \sqrt{3} L_o, \quad [3.13]$$

where $L_o = l\sqrt{N}$ is the mean-square end-to-end distance of the portion of the polymer molecule dissolved in the film, say the polyoxyethylene portion of a nonionic surfactant

molecule; l and N are the length of a fragment unit and their number in the polymer chain. Typical ranges of values of l and N are $0.5 \text{ nm} \leq l \leq 1.5 \text{ nm}$ and $10 \leq N \leq 10^4$ (13, 28), which correspond to a thickness of the polymer layer from a few nanometers to 150 nm. The interfacial area per polymer molecule, $A = 1/\Gamma$, is typically several times larger than l^2 . By combining Eq. [3.13] with Derjaguin's approximation, Eq. [2.3], we obtain the energy of steric interaction between two deformed drops,

$$W^{\text{st}} = 4\pi\Gamma kT \left[r^2 e^{-3/2\tilde{h}^2} + \sqrt{\frac{\pi}{6}} aL_o \times \text{erfc} \left(\sqrt{\frac{3}{2}} \tilde{h} \right) \right] \quad \text{for } h > L_o \sqrt{3} \quad [3.14]$$

$$W^{\text{st}} = \pi r^2 \Gamma kT \left[\frac{\pi^2}{3\tilde{h}^2} + \ln \left(\frac{3\tilde{h}^2}{8\pi} \right) \right] + \pi a \Gamma kT L_o \left[\frac{\pi^2}{3\tilde{h}} \left(1 - \frac{\tilde{h}}{\sqrt{3}} \right) + 2\tilde{h} \left(1 - \ln \sqrt{\frac{3\tilde{h}^2}{8\pi}} \right) - 5.235 \right] \quad \text{for } h < L_o \sqrt{3} \quad \tilde{h} = h/L_o. \quad [3.15]$$

In Fig. 10, the contour plot of the interaction energy between two sterically stabilized drops is shown. Besides the

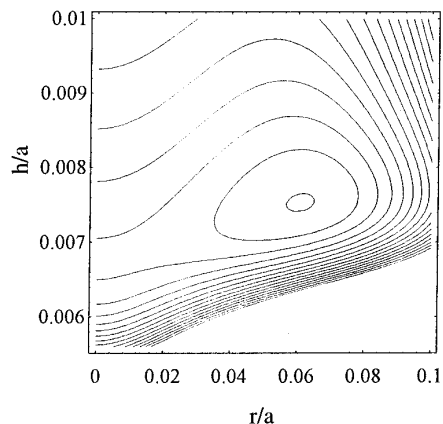


FIG. 10. Contour plot of the interaction energy between two sterically stabilized drops. The parameters used in these calculations are: number of monomer units in a polymer chain $N = 25$, length of a monomer unit $l = 0.6$ nm, $\Gamma = 1.15 \times 10^{-14}$ mol/m² ($A_o = 1.44$ nm²), $L_o = 3$ nm. The remaining parameters are as in Fig. 2b. The energy minimum $W(h_e, r_e)/kT = -31.1$ at $r_e/a = 0.061$ and $h_e/a = 0.0075$ and $W(h^*, 0)/kT = -27.3$ at $h^*/a = 0.0068$. The distance between the contours equals 2 kT.

steric repulsion, the van der Waals and the surface extension energies are taken into account (see Eqs. [2.1], [2.6], and [3.14]). The parameters used in these calculations are number of monomer units in a polymer chain $N = 25$, length of a monomer unit $l = 0.6$ nm, $\Gamma = 1.15 \times 10^{-14}$ mol/m² ($A_0 = 1.44$ nm²), and $L_0 = 3$ nm. These parameters roughly correspond to emulsions stabilized with nonionic surfactant (e.g., alkylpolyoxyethylene) with 25 ethoxy groups. The remaining parameters are the same as in Fig. 2b. The energy minimum $W(h_c, r_c)/kT = -31.1$ at $r_c/a = 0.061$ and $h_c/a = 0.0075$ is deeper compared to the case of nondeformable particles: $W(h^*, 0)/kT = -27.3$ at $h^*/a = 0.0068$.

At theta-conditions, the steric interaction corresponds to a monotonic repulsion and in some aspects resembles the electrostatic repulsion between charged surfaces. The range of steric interaction is proportional to the thickness of the adsorbed layer, $L_0/\sqrt{6}$ in this case (see Ref. (14, p. 304)). Thus the variation of the molecular mass of the polymer leads to an effect similar to that due to the variation of the electrolyte concentration in the case of electrostatic repulsion. For sufficiently thick adsorption layers the van der Waals attraction becomes negligible and the drops interact as nondeformable spheres.

In the case of *good solvents* the interaction energy between two deformed droplets covered with brush layers can be determined by means of Alexander–de Gennes theory (28, 29),

$$f^{\text{st}}(h) = 2kT\Gamma^{3/2}L_g \left[\frac{4}{5} \tilde{h}_g^{-5/4} + \frac{4}{7} \tilde{h}_g^{7/4} - \frac{48}{35} \right]$$

for $h < 2L_g$

$$W^{\text{st}} = \pi r^2 f^{\text{st}}(h) + 4\pi a k T \Gamma^{3/2} L_g^2$$

$$\times [1.37\tilde{h}_g - 0.21 \tilde{h}_g^{11/4} + 3.20 \tilde{h}_g^{-1/4} - 4.36]$$

for $h < 2L_g$, [3.16]

where L_g is the polymer layer thickness in a good solvent,

$$L_g = N(\Gamma l^5)^{1/3}, \quad \tilde{h}_g = h/2L_g. \quad [3.17]$$

A quantitative experimental verification of the Alexander–de Gennes theory was performed by Taunton *et al.* (30), who measured the forces between two polystyrene brush layers in toluene and demonstrated very good agreement between the theory and experiment. The steric interaction in good solvents corresponds to a monotonic repulsion whose range is characterized by the layer thickness L_g . Therefore, the influence of the polymer molecular mass and surface concentration is qualitatively similar to that in the case of theta-solvent considered above. There are, however, some differences between these two cases. For instance, the thick-

ness of the adsorbed layer at theta-conditions L_0 (and the range of steric interactions) does not depend on the interfacial polymer concentration, while in good solvents L_g (and the range of steric interaction) increases with the increase of the polymer adsorption.

The theory and experiment show that with polymers in *poor solvent* one can observe a minimum in the steric interaction energy at separations close to the polymer layer thickness (13, 28). This minimum is due to the attraction between the polymer segments in poor solvent. At smaller separations strong steric repulsion between the adsorbed layers appears. This interesting case can be treated only numerically, e.g., by means of the theory developed by Ploehn and Russel (13, 28).

4. ENERGY OF INTERFACIAL BENDING

The energy contribution caused by the variation of the interfacial curvature is usually studied in connection with the properties of lipid bilayers and microemulsions (31–34). According to Helfrich (31), the bending energy per unit area of a spherical interface can be presented in the form

$$w^c = 2k_c(H - H_0)^2 = B_0H + 2k_cH^2 + 2k_cH_0^2, \quad [4.1]$$

where k_c is the bending elasticity constant, $H = -1/a$ is the interfacial curvature and $H_0 = -1/R_0$ is the spontaneous curvature (a and R_0 are the respective radii of curvature), and $B_0 = -4k_cH_0$ is the interfacial bending moment of a flat interface (see, e.g., Ref. (33)). Then the corresponding contribution to the droplet deformation energy can be found (3) as a difference of the droplet curvature energy after and before the film formation, respectively:

$$W^c = -2\pi r^2 B_0 H \left(1 - \frac{H}{2H_0} \right) \quad (r/a)^2 \ll 1. \quad [4.2]$$

For emulsion interfaces k_c was measured (35) to be on the order of the thermal energy, kT . The theoretical calculations (36) show that usually $|B_0|$ is on the order of 5×10^{-11} N for emulsion interfaces. If such is the case one can estimate that for emulsion systems H_0 is on the order of nm⁻¹. Since the curvature of the emulsion droplets, H , is typically several orders of magnitude smaller ($H \sim 10^{-3}$ nm⁻¹), the second term in the parentheses in Eq. [4.2] can be neglected (the same is true for the term with the Gaussian curvature which has been neglected in Eq. [4.1] from the very beginning). Thus one obtains

$$W^c = -2\pi r^2 B_0 H \quad (r/a)^2 \ll 1, \quad |R_0/a| \ll 1. \quad [4.3]$$

Assuming $r \approx a/50$ from [4.3] one obtains $|W^c| = (\pi/1250)|B_0|a$. Then with $a = 3 \times 10^{-5}$ cm and the above value of $|B_0|$ one calculates $|W^c| \approx 10 kT$. In other words, the bending effects can be important for the interaction between submicrometer emulsion droplets.

It should be noted that the sign of the curvature H and the bending moment B_0 is a matter of convention. It is determined by the definition of the direction of the unit surface normal \mathbf{n} (from the oil phase toward the aqueous phase or the opposite). The general rule is that positive B_0 tends to bend the interface around the inner phase (the phase for which \mathbf{n} is an outer normal). For the emulsion systems, studied in Refs. (36), B_0 always tends to bend around the oil phase (this is an absolute property, independent on the definition of the direction of \mathbf{n}). This holds when B_0 is dominated by the double layer and van der Waals surface forces. If such is the case, the interfacial bending moment will facilitate the formation of flat film between two aqueous droplets in oil and will oppose the formation of flat film between two oil droplets in water. Note also that the sign of the product B_0H (and W^c) is independent on the choice of the direction of \mathbf{n} . In the case considered above $W^c < 0$ for aqueous droplets in oil, whereas $W^c > 0$ for oil droplets in water. The bending energy contribution can vary with the variation of the experimental conditions (electrolyte concentration for ionic surfactants or temperature for nonionic surfactants).

The bending energy is known to be important for interfaces of very high curvature like microemulsion droplets or nuclei of droplets. This is the reason why the conclusion, based on Eq. [4.3], that the interfacial bending energy is significant for the interaction between emulsion droplets of micrometer size may seem quite surprising. Nevertheless, the effect exists and is due to the fact that the bent area increases faster ($r^2 \propto a^2$) than the bending energy per unit area decreases ($H \propto 1/a$) when the droplet radius, a , increases, cf., Eq. [4.3].

The bending effects are also important in emulsion systems of low interfacial tension. Upon stirring in such systems simultaneous formation of both emulsion and microemulsion droplets can be observed (Fig. 11). One can expect that $B_0H < 0$ facilitates the formation of stable droplets (indeed, $W_c > 0$ and the bending moment opposes the deformation of the droplets). It is natural to assume that the latter condition is fulfilled for the microemulsion droplets, for which the bending effect is especially important because of their high curvature. Hence in Fig. 11a $B_0H < 0$ for both micro- and miniemulsion droplets; consequently the bending energy will stabilize (prevent flat film formation upon collision) the droplets of both sizes.

On the contrary, H has opposite signs for micro- and miniemulsion droplets in the configuration depicted in Fig. 11b, viz. again $B_0H < 0$ for the microemulsion droplets,

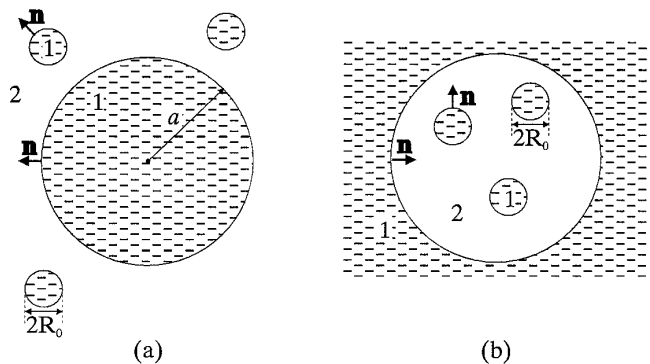


FIG. 11. Sketch of a miniemulsion drop in coexistence with smaller microemulsion droplets in the continuous phase (a) or in the discontinuous phase (b).

whereas $B_0H > 0$ for the larger miniemulsion drops. Consequently, the interfacial bending moment will favor the formation of a plane parallel film between two colliding miniemulsion drops and will facilitate their flocculation. This consideration is in a qualitative agreement with the experimentally observed correlation between the types of microemulsion and miniemulsion formed at given conditions (37). According to Davies and Rideal (38), after homogenization both types of miniemulsions (oil-in-water and water-in-oil) are formed. The emulsion which “survives” is the one containing the more slowly coalescing droplets. The curvature effects will facilitate substantial deformation and stronger attraction (flocculation and coalescence) of the emulsion drops containing microemulsion droplets inside. In contrast, the bending energy will prevent the deformation of the drops in the reverse emulsion. Therefore, it can be expected that the emulsion containing microemulsion droplets in the continuous phase will be more stable and will survive, as observed experimentally (37). One should note that the depletion attraction (due to the microemulsion droplets) tends to destabilize the latter emulsion, but probably it is of less importance (in comparison with the curvature effects) for that system.

5. CONCLUSIONS

The general approach for studying the interaction between deformable emulsion droplets of micrometer and submicrometer size, proposed in Ref. (4), is applied to study the effect of a variety of interparticle forces. It allows taking into account not only the conventional electrostatic and van der Waals forces, but also the non-DLVO surface forces: depletion, oscillatory, steric, etc.

The main new results of this study are the following:

(1) The formation of equilibrium thin film between two similar colliding emulsion droplets happens above some

threshold values of the electrolyte concentration and droplet size; see Figs. 3a and 4a.

(2) At high concentration of surfactant micelles, the oscillatory structural forces may lead to the appearance of several minima in the potential energy surface (Fig. 8), corresponding to different number of micellar layers in the film between the droplets. The relative magnitude of the interaction energy in these minima, as well as the energy barriers for transition between them, are very sensitive to the conditions. These effects can be quantified by means of Eqs. [3.6]–[3.9].

(3) At low micelle volume fraction the oscillatory forces degenerate into the attractive depletion forces, which strongly favor the droplets' deformation upon collision; see Figs. 7a and 7b. An important conclusion is that at high volume fractions the micelles (or other small colloidal particles) stabilize emulsions due to the energy barriers produced by the oscillatory structural forces; in contrast, at low volume fraction the micelles destabilize the dispersions due to the depletion attraction.

(4) The contribution of the interfacial bending energy into the total droplet–droplet interaction is studied quantitatively; see Eq. [4.3]. The magnitude of the bending energy is on the order of $10 kT$ and corresponds to droplet–droplet attraction in water-in-oil emulsions and to droplet–droplet repulsion in oil-in-water emulsions. The bending energy effect can in principle explain why an emulsion containing microemulsion droplets in the continuous phase is more stable than an emulsion containing microemulsion droplets in the disperse phase.

The calculations show that for weak attraction the droplets interact as nondeformed spheres. For stronger attraction (larger Hamaker constant and/or electrolyte concentration, lower interfacial tension, depletion effects, etc.) a plane parallel film forms between the droplets, whose thickness and radius can be calculated. The magnitude of the attractive energy between two deformed drops is usually much larger than that between two nondeformed spheres of the same size, Hamaker constant, surface potential, etc., which leads to stronger flocculation.

In summary, the present article complements the general concept from Ref. (4) with a thorough examination of the impact of the interfacial stretching and bending properties, and the various surface forces on the droplet–droplet interaction in emulsions. The results may find application for interpretation of data for various phenomena in emulsions obtained by light scattering, phase behavior, rheological and osmotic pressure measurements, etc.

ACKNOWLEDGMENTS

This study was supported by the Bulgarian Ministry of Science and Higher Education. We are indebted to Ms. M. Paraskova for typing the manuscript.

REFERENCES

- Denkov, N. D., Petsev, D. N., and Danov, K. D., *J. Colloid Interface Sci.* **176**, 189 (1995).
- Kralchevsky, P. A., and Ivanov, I. B., *Chem. Phys. Lett.* **121**, 111 and 116 (1985).
- Danov, K. D., Petsev, D. P., Denkov, N. D., and Borwankar, R., *J. Chem. Phys.* **99**, 7179 (1993).
- Denkov, N. D., Petsev, D. N., and Danov, K. D., *Phys. Rev. Lett.* **71**, 3326 (1993).
- Danov, K. D., Denkov, N. D., Petsev, D. N., and Borwankar, R., *Langmuir* **9**, 1732 (1993).
- Aronson, M. P., and Princen, H., *Nature* **296**, 370 (1980); Aronson, M. P., and Princen, H., *Colloids Surf.* **4**, 173 (1982).
- Hofman, J. A. M. H., and Stein, H. N., *J. Colloid Interface Sci.* **147**, 508 (1991).
- Denkov, N. D., Kralchevsky, P. A., Ivanov, I. B., and Vassilieff, C. S., *J. Colloid Interface Sci.* **143**, 157 (1991).
- Bibette, J., Roux, D., and Nallet, F., *Phys. Rev. Lett.* **65**, 2470 (1990); Bibette, J., Roux, D., and Pouligny, B., *J. Phys. II France* **2**, 401 (1992).
- Verwey, E. J. W., and Overbeek, J. Th. G., "Theory and Stability of Lyophobic Colloids." Elsevier, Amsterdam, 1948.
- Derjaguin, B. V., Churaev, N. V., and Muller, V. M., "Surface Forces." Nauka, Moscow, Plenum/Consultants Bureau, New York, 1987.
- Derjaguin, B. V., "Theory of Stability of Colloids and Thin Liquid Films." Plenum/Consultants Bureau, New York, 1989.
- Russel, W. B., Saville, D. A., and Schowalter, W. R., "Colloidal Dispersions." Cambridge Univ. Press, Cambridge, 1989.
- Israelachvili, J. N., "Intermolecular and Surface Forces," 2nd ed., Academic Press, London, 1991.
- Visser, J., *Adv. Colloid Interface Sci.* **3**, 341 (1972).
- Kralchevsky, P. A., Danov, K. D., and Ivanov, I. B., in "Foams: Theory, Measurements and Applications" (R. K. Prud'homme, Ed.), Elsevier, Amsterdam, in press.
- Aronson, M. P., *Langmuir* **5**, 494 (1989).
- Tadros, Th. V., and Vincent, B., in "Encyclopedia of Emulsion Technology" (P. Becher, Ed.), Vol. 1, p. 130. Dekker, New York, 1983.
- Carnahan, N. F., and Starling, K. E., *J. Chem. Phys.* **51**, 636 (1969).
- Russel, W. B., and Benzing, D. W., *J. Colloid Interface Sci.* **83**, 163 (1981); Benzing, D. W., and Russel, W. B., *J. Colloid Interface Sci.* **83**, 178 (1981).
- Nikolov, A. D., and Wasan, D. T., *J. Colloid Interface Sci.* **134**, 1 (1989); Nikolov, A. D., Kralchevsky, P. A., Ivanov, I. B., and Wasan, D. T., *J. Colloid Interface Sci.* **134**, 13 (1989).
- Nikolov, A. D., Wasan, D. T., Denkov, N. D., Kralchevsky, P. A., and Ivanov, I. B., *Prog. Colloid Polym. Sci.* **82**, 87 (1990); Wasan, D. T., Nikolov, A. D., Kralchevsky, P. A., and Ivanov, I. B., *Colloids Surf.* **67**, 139 (1992).
- Richetti, P., and Kekicheff, P., *Phys. Rev. Lett.* **68**, 1951 (1992); Parker, J. L., Richetti, P., Kekicheff, P., and Sarman, S., *Phys. Rev. Lett.* **68**, 1955 (1992).
- Denkov, N. D., and Kralchevsky, P. A., *Prog. Colloid Polym. Sci.* **98**, 18 (1995).
- Karlström, G., *Chem. Scripta* **25**, 89 (1985).
- Henderson, D., *J. Colloid Interface Sci.* **121**, 486 (1988).
- Dolan, A. K., and Edwards, S. F., *Proc. Royal Soc. London, Ser. A* **347**, 509 (1974).
- Ploehn, H. J., and Russel, W. B., *Adv. Chem. Eng.* **15**, 137 (1990).
- Alexander, S. J., *Physique* **38**, 983 (1977); de Gennes, P. G., *Adv. Colloid Interface Sci.* **28**, 189 (1987).

30. Taunton, H. J., Toprakciaglu, C., Fetters, L. J., and Klein, J., *Macromolecules* **23**, 571 (1990).
31. Helfrich, W., *Z. Naturforsch C* **30**, 510 (1974).
32. de Gennes, P. G., and Taupin, C., *J. Phys. Chem.* **86**, 2304 (1982).
33. Kralchevsky, P. A., Eriksson, J. C., and Ljunggren, S., *Adv. Colloid Interface Sci.* **48**, 19 (1994).
34. Petrov, A. G., and Bivas, I., *Progr. Surf. Sci.* **16**, 389 (1984).
35. Binks, B. P., Kellay, H., and Meunier, J., *Europhys. Lett.* **16**, 53 (1991); Binks, B. P., Meunier, J., and Langevin, D., *Prog. Colloid Polym. Sci.* **79**, 208 (1989).
36. Gurkov, T. D., Kralchevsky, P. A., and Ivanov, I. B., *Colloids Surf.* **56**, 119 (1991); Kralchevsky, P. A., Gurkov, T. D., and Ivanov, I. B., *Colloids Surf.* **56**, 149 (1991).
37. Binks, B. P., *Langmuir* **9**, 25 (1993).
38. Davies, J., and Rideal, E., "Interfacial Phenomena." Academic Press, New York, 1963.